

1 **Structure of the high molecular weight exopolysaccharide**
2 **produced by *Bifidobacterium animalis* subsp. *lactis* IPLA-R1 and**
3 **sequence analysis of its putative *eps* cluster**

4

5 Shaun Leivers^a, Claudio Hidalgo-Cantabrana^b, Glenn Robinson^a, Abelardo
6 Margolles^b, Patricia Ruas-Madiedo^b and Andrew P. Laws^{a*}

7

8

9 ^a Department of Chemical and Biological Sciences, University of Huddersfield,
10 Queensgate, Huddersfield, HD1 3DH, United Kingdom

11 ^b Instituto de Productos Lácteos de Asturias, Consejo Superior de Investigaciones
12 Científicas (IPLA-CSIC), Carretera de Infiesto s/n, 33300 Villaviciosa, Asturias,
13 Spain

14

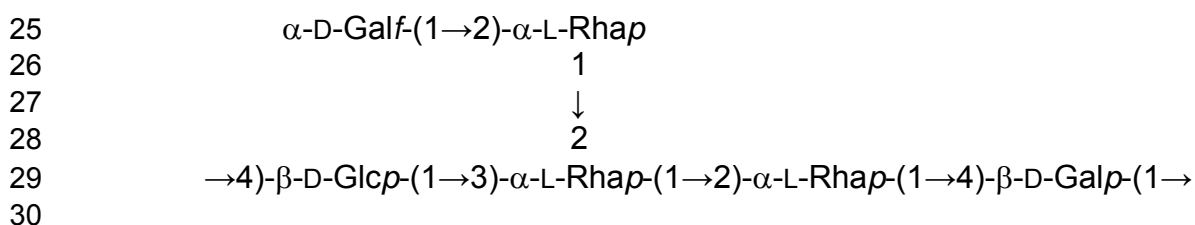
15 *Corresponding Author: Tel+44(1484)472668; Fax +44(1484)472182;

16 E-mail address a.p.laws@hud.ac.uk

17

18 **Abstract**

19 The bile adapted strain *Bifidobacterium animalis* subsp. *lactis* IPLA-R1
20 secretes a high molecular weight exopolysaccharide (HMW-EPS) when grown on
21 the surface of agar-MRSC. This EPS is composed of L-rhamnopyranosyl, D-
22 glucopyranosyl, D-galactopyranosyl and D-galactofuranosyl residues in the ratio of
23 3:1:1:1. Linkage analysis and 1D and 2D-NMR spectroscopy were used to show that
24 the EPS has a hexasaccharide repeating unit with the following structure:



31 Treatment of the EPS with mild acid cleanly removed the terminal D-
32 galactofuranosyl residue. The *eps* cluster sequenced for strain IPLA-R1 showed high
33 genetic homology with putative *eps* clusters annotated in the genomes of strains
34 from the same species. It is of note that several genes coding for rhamnose-
35 precursors are present in the *eps* cluster, which could be correlated with the high
36 percentage of rhamnose detected in its EPS repeated unit.

37

38 **Keywords:**

39 *Bifidobacterium*, exopolysaccharide, EPS structure, *eps* cluster, glycosyltransferase

40

41 1. Introduction

42 Bifidobacteria are Gram-positive non-spore forming, non motile, non
43 filamentous rods which can display various shapes, the most typical one is bifurcated
44 with spatulated extremities. They are strict anaerobes, with high G+C content
45 belonging to the phylum *Actinobacteria* and they are normal constituents of a healthy
46 gut microbiota of animals. Currently more than 30 species are included in the genus
47 *Bifidobacterium*, whilst most abundant in the human gastrointestinal tract are *B.*
48 *adolescentis*, *B. angulatum*, *B. bifidum*, *B. breve*, *B. catenulatum*, *B. longum* and *B.*
49 *pseudocatenulatum*. Bifidobacteria are regarded as probiotic microorganisms and
50 are increasingly being consumed as supplements in foods or in pharmaceutical
51 formulations, to promote a healthy gut microbiota balance. The species most often
52 found in functional dairy products is *Bifidobacterium animalis* subsp. *lactis*¹.

53 Probiotics have been defined as “live microorganisms, which when
54 administered in adequate amounts confer a health benefit on the host”². The degree
55 of scientific evidence of probiotic effect in humans is scarce since most of these
56 beneficial claims are based on the extrapolation of results of *in vitro* and animal
57 model experiments. There are only a limited number of reports showing efficacy of a
58 few specific probiotic strains in human intervention studies. Several meta-analyses
59 collecting clinical evidence have demonstrated probiotic efficacy in alleviating lactose
60 intolerance, antibiotic associated diarrhoea, atopic allergy in infants and some
61 inflammatory bowel diseases^{3,4}. One of the potential mechanisms by which probiotic
62 bacteria can elicit their health benefits is through the surface molecules such as the
63 exopolysaccharides (EPS). These biopolymers are exocellular carbohydrates that
64 can be: covalently linked to bacterial surface forming a capsule; they can be non-

65 covalently associated with the surface or be totally secreted. Several health benefits
66 have been *in vitro* attributed to EPS, such as cholesterol lowering capability,
67 prebiotic effect and modulating the immune response⁵. Bifidobacteria isolated from
68 human intestinal origin are able to synthesise EPS composed of more than one type
69 of monosaccharide^{6,7}. Regarding the putative role of EPS produced by bifidobacteria
70 in the gut environment, it has been reported that bile salts induce their synthesis in
71 some strains of *B. animalis* subsp. *animalis*⁸. Thereby, it seems that these polymers
72 could have a protective role for the producing bacteria. This property is interesting for
73 orally delivered strains since it could help bifidobacteria to survive the challenges,
74 mainly acidic conditions and high concentration of bile salts that they will encounter
75 on their transit from the mouth to the small intestine. In the large intestine, EPS-
76 producing bifidobacteria will meet a complex ecosystem inhabited by a vast number
77 of microorganisms. Salazar and co-workers have reported that a number EPS
78 isolated from bifidobacteria have an ability to *in vitro* modulate the composition of
79 human intestinal microbiota⁹. A similar effect has been recently shown *in vivo* using
80 rats fed with the EPS-producing strain *B. animalis* subsp. *lactis* IPLA-R1¹⁰.
81 Additionally, the EPS produced by this strain was able to *in vitro* counteract the
82 cytotoxic effect of bacterial toxins upon colonocyte-like Caco-2 cells. This EPS-
83 fraction was analysed by size exclusion chromatography coupled with multi-angle
84 laser light scattering detection (SEC-MALLS) and it was found a distribution of three
85 molecular weight peaks differing in size¹¹.

86 Whilst there are a number of reports of EPS producing bifidobacteria, very
87 little work has been undertaken to fully characterise the EPS that they produce, as
88 well as their genetic determinants. The structures of the EPS produced by *B. bifidum*
89 BIM B-465¹² and *B. longum* JBL05¹³ both of human origin, have recently been

90 reported. But, as far as we know, the functional characterization of genes coding for
91 enzymes involved in EPS-synthesis in *Bifidobacterium* has not been undertaken to
92 date. A recent comparative analysis of bifidobacterial genomes shows that the
93 presence of putative *eps* clusters seems to be an ubiquitous character in this genus¹⁴.
94 Thereby, the aim of this study was to analyse the structure of the EPS produced by
95 *B. animals* subsp. *lactis* IPLA-R1, a promising strain with probiotic potential, and to
96 analyse the sequence of the putative *eps* cluster coding for proteins involved in the
97 synthesis of this polymer.

98

99 **2. Results and Discussion**

100 **2.1. Structure of the HMW-EPS polymer synthesised by strain IPLA-R1**

101 The crude-EPS sample purified from *B. animals* subsp. *lactis* IPLA-R1 had a
102 protein content of 3.9% and the molecular weight distribution was similar to that
103 previously reported by SEC-MALLS¹¹: a high molecular weight fraction (HMW) with
104 average molecular weight of 3.5×10^6 Da, a middle weight EPS (3.0×10^4 Da) and a
105 low molecular weight EPS (4.9×10^3 Da). Dialysis of the crude-EPS sample against
106 a 100 kDa cellulose acetate membrane separated the HWM-EPS, which was
107 isolated in the retentate with reasonable purity. By SEC-MALLS separation, the
108 average molecular weight of the HMW-EPS in the retentate was measured as $3.5 \times$
109 10^6 Da. The purity of the HMW-EPS was also determined by comparison of the
110 anomeric region of the NMR spectra before (Fig 1a) and after dialysis (Fig1b), only a
111 small amount of additional material (assumed to be middle weight EPS) was present.
112 Six anomeric protons appear in the anomeric region of the ¹H NMR spectrum of the
113 HMW-EPS suggesting that the repeating unit is a hexasaccharide; from this point

114 forward, the anomeric signals of the individual monomers are arbitrarily labelled as **A**
115 to **F**, in decreasing order of their chemical shifts.

116 The results of monomer analysis and determination of the absolute
117 configuration of the monomers indicate that the polysaccharide is composed of L-
118 rhamnose, D-galactose and D-glucose in a molar ratio of 2.85:1.97:1. After
119 performing linkage analysis, five unique methylated alditol acetates were obtained
120 including: a 1,4,5-tri-*O*-acetyl-2,3,6-tri-*O*-methylglucitol (from 1,4-Glcp); a 1,4,5-tri-*O*-
121 acetyl-2,3,6-tri-*O*-methylgalactitol (from 1,4-Galp); a 1,2,5-tri-*O*-acetyl-3,4-di-*O*-
122 methylrhamnitol (from 1,2-Rhap); a 1,2,3,5-tetra-*O*-acetyl-4-*O*-methylrhamnitol (from
123 1,2,3- Rhap); and a 1,4-di-*O*-acetyl-2,3,5,6-tetra-*O*-methylgalactitol (from t-Galf).

124 The structure of the HMW-EPS was determined using the results of the
125 linkage analysis and by inspection of a range of 1D and 2D-NMR spectra including:
126 ^1H - ^1H COSY; ^1H - ^1H TOCSY; ^1H - ^{13}C HMBC; ^1H - ^{13}C HSQC and ^1H - ^{13}C HSQC-
127 TOCSY spectra. The first thing to note is the anomeric configuration of each of the
128 monomers, for monomers **A** to **D** this was determined by measurement of the
129 magnitude of the $^1J_{\text{C-H}}$ coupling constant for the anomeric signals **A** (173 Hz), **B** (175
130 Hz), **C** (176 Hz) and **D** (175 Hz) these values are all greater than 170 Hz and
131 identifies each as having α -linkages. The anomeric configuration of the two
132 remaining monomers (**E** and **F**) was determined by measurement of the $^3J_{\text{H1-H2}}$
133 coupling constants which were both greater than 8 Hz identifying that **E** and **F**
134 residues have β -linkages.

135 The position of the remaining proton resonances (H-2 to H-6) was determined
136 using a combination of the COSY and TOCSY spectra. On the ^1H - ^1H TOCSY
137 spectrum (120 ms, data not shown) there are cross peaks from the anomeric protons
138 of residues **A**, **B** and **C** to H-4 and, in the methyl region, from H-6 to H-3, identifying

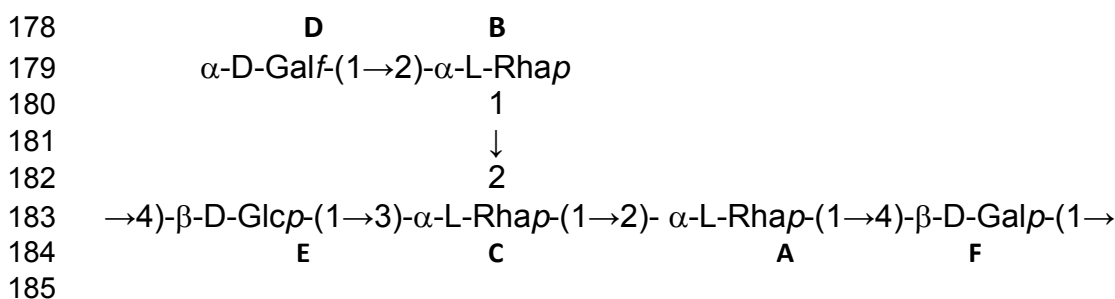
139 **A, B** and **C** as the rhamnose monomers. For residues **D, E** and **F** cross peaks on the
140 COSY and TOCSY spectra identified the positions of H-1 through to H-4. The exact
141 positions of H-5- and H-6 were not easily determined as there is poor transmission of
142 coupling beyond H-4. The position of the remaining resonances was obtained from
143 inspection of a ^{13}C Dept spectrum and from the HQSC spectrum. On the ^{13}C Dept
144 spectrum, the C-6 resonances are located together at approximately 60 ppm. Once
145 all the cross-peaks on the HSQC spectrum for C1/H1 to C4/H4 and for C6/6 had
146 been assigned (Fig 2) the three remaining cross peaks must be those belonging to
147 C/H-5s. Finally, these were assigned to individual monomers by cross reference to a
148 HSQC-TOCSY spectrum. As the structure does not have any glycosidic links
149 involving the hydroxyls at C6, our failure to assign the individual H-6 residues to **D, E**
150 and **F** has no consequence for the characterisation of the EPS. For clarity, the
151 resonance position for the ^1H signals and ^{13}C signals (H2 to H5 and C2 to C5) are
152 indicated on the ^1H - ^{13}C HSQC spectrum (Fig 2a, anomeric signals appear on the
153 inset Fig 2b) the anomeric proton resonances are also indicated on the ^1H - ^1H
154 NOESY spectrum (Fig 3) and the combined chemical shift data for the complete
155 repeating unit is presented in Table 1.

156 The very low field chemical shift values for H-2, H-3 and the H-4 resonances
157 of residue **D**, combined with the loss of this residue under mildly acidic conditions
158 (see discussion below), is evidence for residue **D** being the terminal Galf. This would
159 leave residues **E** and **F** as the 1→4 linked hexoses. One way of differentiating
160 between galacto- and glucopyranoses is from inspection of the chemical shifts for
161 their H-4 resonances: for a galactose H-4 is shifted substantially to lower field than
162 that of a glucose regardless of the anomeric configuration and linkage. Data
163 collected from assignments for lactic acid bacteria (LAB) EPS structures show that

164 the H-4 resonances for galactose lie in the range 4.30-3.85 δ whilst those for glucose
165 lie in the range 3.45 -3.75 δ ¹⁵. The chemical shift for **E** H-4 (3.61) and that for **F** H-4
166 (4.39) implies that **E** is the glucopyranose sugar and **F** is the galactopyranose.

167 Information regarding the sequence of the sugar residues in the repeating unit
168 was obtained from examination of the NOESY spectrum (Fig 3) and the anomeric
169 region of the HMBC spectrum (not shown). On the NOESY spectrum there are
170 strong inter residue NOEs between: **A** H-1 and **F** H-4, **B** H-1 and **C** H-2, **D** H-1 and **B**
171 H-2, **E** H-1 and **C** H-3, and **F** H-1 and **E** H-4; identifying **A**(1 \rightarrow 4)**F** , **B**(1 \rightarrow 2)**C**,
172 **D**(1 \rightarrow 2)**B**, **E**(1 \rightarrow 3)**C** and **F**(1 \rightarrow 4)**E** linkages. On the HMBC spectrum inter-residue
173 couplings are observed between: **A** H-1 and **F** H-4, **B** H-1 and **C** H-2, and **D** H-1 and
174 **B** H-2, matching the NOE signals and, additionally, a cross peak is observed
175 between **C** H-1 and **A** H-2.

176 Using a combination of the results for the linkage analysis and the NMR
177 identifies the structure for the repeating unit as:



186 This is a novel structure and differs to those of the EPS structures that have been
187 reported for *B. bifidum* BIM B-465¹² and *B. longum* JBL05¹³ and is also different to
188 the EPSs that have been isolated and characterised from LAB¹⁵.

189

190 **Mild acid catalysed hydrolysis of the HMW EPS**

191 It is well known that glycosidic links to Galf residues are hydrolysed in acidic
192 solution¹⁶. Treatment of the HMW-EPS with a dilute solution of trifluoroacetic acid in

193 an NMR tube caused the loss of the *Galf* residue which we were able to monitor over
194 time (Fig 4). Within a period of 8 hours the anomeric signal, from residue **D**, reduced
195 in intensity and ultimately merged with the spectral noise. It seems that the EPS
196 IPLA-R1 could have a protective role during the transit of the producing bacteria
197 through the upper part of the intestinal tract¹⁰. However, in the *in vivo* situation this
198 *Galf* residue could be either partially or totally lost. Thereby, care will be needed in
199 attempting to correlate EPS structure with biological activity measured *in vitro*, since
200 the passage through the gastrointestinal tract could modify its composition.

201

202 **2.2 Putative *eps* cluster of *B. animalis* subsp. *lactis* IPLA-R1**

203 A fragment of 54,259 bp containing the putative *eps* cluster of the strain *B.*
204 *animalis* subsp. *lactis* IPLA-R1 was sequenced and the putative function of coded
205 proteins has been studied by homology comparison with sequences held in the
206 GenBank database. A high genetic homology was detected among the putative *eps*
207 cluster of our strain IPLA-R1 and those of the five *B. animalis* subsp. *lactis* whose
208 genomes are currently available (data not shown). As expected, the functional maps
209 were almost identical among the six strains; this was not surprising since it has been
210 shown that there is a scarce inter-strain genetic variability within this *Bifidobacterium*
211 species¹⁷.

212 The best characterised *eps* clusters, either by homology comparison or by
213 functional studies, are those of LAB and, in fact, a functional structure has been
214 found among these clusters¹⁸. Taking into account this functional structure, several
215 proteins involved in the synthesis of EPS have been found in the *eps* cluster of *B.*
216 *animalis* subsp. *lactis* IPLA-R1 (Figure 5). This is the case of glycosyltransferases

217 (GTF), priming-GTF (p-GTF), genes involved in export of repeated unit, its
218 polymerization and chain length determination, as well as mobile elements
219 (transposase and insertion sequences (IS)). However, no gene regulators have been
220 found although this function could be played by proteins with unknown function
221 within the cluster or others outside it. It is also surprising that a number of membrane
222 proteins are present in the bifidobacterial *eps* cluster. Another remarkable feature in
223 the IPLA-R1 *eps* cluster is the presence of two p-GTF, as previously denoted for *B.*
224 *longum* subsp. *longum* NCC2705¹⁹ and for the other *B. animalis* subsp. *lactis*
225 strains¹⁴. This enzyme catalyses the transfer of an activated sugar to the lipid carrier
226 C55, being the first step in the synthesis of the repeated unit that build the polymer.
227 In *B. animalis* subsp. *lactis* IPLA-R1, one of the p-GTF was located in the 5' end
228 (annotated as “undecaprenyl-phosphate sugar phosphotraferease”) and the second
229 one was located down-stream (annotated as galactosyl transferase *CpsD*). The
230 nucleotide sequences of the two p-GTFs of the strain IPLA-R1 were different to the
231 corresponding homologues of the type-strain DSM10140. In addition, in the strain
232 IPLA-R1 the change in the nucleotide sequence of *cpsD*, but not that of the
233 undecaprenyl-phosphate sugar phosphotraferease gene, led to a modification in
234 the translated amino acid. However, we do not know if this different amino acid
235 residue could modify the function of this p-GTF and thereby, influence the synthesis
236 of the EPS in IPLA-R1 strain. Variations in the nucleotide sequence were also
237 detected in the transposase IS204/IS1001/IS1096/IS1165 located at the 3'end,
238 probably due to gain or loss of nucleotides in this mobile element during each
239 transposition.

240 In relation to the structure of the HMW-EPS IPLA-R1 determined in this study,
241 it is worth mentioning the presence of genes coding for proteins involved in the

242 biosynthesis of rhamnose precursors in the putative *eps* gene cluster of this strain,
243 which could correlate with the high rhamnose content (50%) of its hexasaccharide
244 repeated unit. Normally, in LAB strains, the content of rhamnose does not exceed
245 that of the other two common EPS monosaccharides: glucose and galactose. An
246 exception is the strain *Lactobacillus rhamnosus* RW9595M whose glucose:
247 galactose: rhamnose ratio is 2:1:4²⁰ and it also presents in its *eps* cluster rhamnose-
248 precursor biosynthesis genes²¹. Additionally, in EPS isolated from intestinal strains
249 the content of rhamnose was higher (52%) than in those isolated from foods (28%)⁷.
250 In this regard, the *in silico* comparative analysis of five bifidobacteria species shows
251 that rhamnose-precursor biosynthesis genes are present in three out of the five
252 species, showing a high degree of protein homology (data not shown). These facts
253 suggest that the high presence of rhamnose in intestinal EPS could play a role in this
254 ecological niche, which deserves future investigation.

255 **3. Experimental**

256 **3.1. Bacterial growth and purification of the HMW-EPS**

257 The growth conditions and purification of the crude-EPS from strain *B. animalis*
258 subsp. *lactis* IPLA-R1 (previously named A1dOxR) have previously been
259 described¹¹. In short, bacterial biomass grown in an anaerobic chamber [MG500
260 (Down Whitley Scientific, West Yorkshire, UK): 80% (v/v) N₂, 10% CO₂, 10% H₂] at
261 37°C for 5 days on the surface of agar-MRSC [MRS (Biokar Diagnostics, Beauvais,
262 France) + 0.25% L-cysteine (Sigma Chemical Co. St. Louis, MO, USA)] was
263 collected with water. The bacterial suspension was mixed with 1 volume of 2M
264 NaOH and the crude-EPS from the cell-free supernatant was precipitated with 2
265 volumes of chilled-absolute ethanol for 48 h at 4°C. The precipitated fraction was

266 resuspended in ultra-pure water, dialysed in 12-14 kDa MWCO cellulose membranes
267 (Sigma) against water for 3 days at 4°C and finally freeze-dried to obtain the EPS-
268 crude fraction.

269 A pure sample of the high molecular weight (HMW)-EPS from the crude-EPS
270 fraction isolated from *B. animals* subsp. *lactis* IPLA-R1 was obtained by dialysis as
271 follows. A crude-EPS sample (25 mg) was dissolved in distilled water (10 mL) with
272 gentle heating (less than 50°C) and the HMW material was isolated in the retentate
273 (about 10 mL), after dialysis (Spectra/Por Float-A-Lyser 100 KDa MWCO, Sigma) for
274 72 hours at 4°C against three changes of distilled water per day. The content of the
275 dialysis membrane were freeze dried to provide HMW-EPS.

276 The purity of the HMW-EPS was determined by SEC-MALLS and NMR analysis.
277 For SEC-MALLS, solutions of EPS in deionised water (1 mg mL⁻¹) were prepared
278 and left for 24 h to completely dissolve. Samples (100 µl) were injected onto an
279 analytical SEC system comprising three columns Aquagel-OH 40, 50 and 60 (15 µm
280 particle size, 25 cm x 4 mm, Varian, Oxford, UK) connected in series. The neutral
281 analytes were eluted with deionised water flowing at 1 mL min⁻¹. The concentration
282 of the EPS fractions eluting from the column were determined by a differential
283 refractometer (Optilab rEX, Wyatt technology, Santa Barbara, USA) and the weight
284 average molecular weight was measured using a Dawn-EOS MALLS operating with
285 a 690 nm laser (Wyatt technology, Santa Barbara).

286 **3.2. Monomer composition and linkages of the HMW-EPS**

287 The monomer composition of the HMW-EPS was determined after acid
288 hydrolysis by HPAEC-PAD. The HMW-EPS (1 mg mL⁻¹) was treated with 2M TFA
289 (120°C for 2 h) and the identity of the released monomers was determined using

290 high performance anion exchange chromatography (HPAEC) on a Dionex BioLC
291 system (Sunnyvale CA, USA) equipped with a CarboPac PA20 column (150 mm x 3
292 mm). Monomers were eluted using a sodium 10 mM hydroxide mobile phase at a
293 flow rate of 0.5 mL min⁻¹ and detected using a pulsed amperometric detector (PAD)
294 ED50 (Dionex) operating with a dual potential waveform. The ratio of monomers was
295 determined by comparison of the detector response to calibration standards of the
296 individual monomers (galactose, glucose and rhamnose, 5-100 ppm). The absolute
297 configurations of monosaccharides were determined by conversion to their butyl
298 glycosides using the procedure described by Gerwig et al²².

299 For linkage analysis, the HMW-EPS was permethylated using the procedures
300 described by Stellner et al²³. The methylated-polysaccharide was hydrolysed by
301 treatment with 2M TFA (120 °C for 2 h) and the methylated monosaccharides
302 converted to their corresponding methylated alditol acetates. The identity of the
303 variously methylated alditol acetates was determined by GLC-MS and by analysis of
304 the individual fragmentation patterns observed in the MS. GLC-MS analyses were
305 performed on an Agilent 7890A GC system (Santa Clara, CA, USA) coupled to an
306 Agilent 5675c quadrupole MS. The samples were eluted from a HP-5 column (30 m
307 x 0.25 mm-id, 0.25 µm film) using helium as carrier (9 psi, flow rate 1 mL min⁻¹) and
308 using the following temperature programme: start temperature 155°C, hold time 1
309 min, and a final column temperature of 195°C reached via a rising gradient of 0.75°C
310 min⁻¹.

311 **3.3. NMR structure of the HMW-EPS**

312 NMR spectra were recorded for HWM-EPS samples that were dissolved (10
313 mg mL⁻¹) directly in D₂O (Goss Scientific Instruments Ltd., Essex, UK). NMR spectra
314 were recorded at a probe temperature of 70°C. The elevated temperature was

315 initially chosen as it shifted the HOD signal to higher field, into a clear region of the
316 spectrum. The higher temperature also increased spectral resolution by reducing the
317 sample viscosity. All of the NMR spectra were recorded on a Bruker Avance 500.13
318 MHz ^1H (125.75 MHz ^{13}C) spectrometer (Bruker-biospin, Coventry, UK) operating
319 with Z-field gradients where appropriate, and using Bruker's pulse programs.
320 Chemical shifts are expressed in ppm relative to either internal or external acetone; δ
321 2.225 for ^1H and δ 31.55 for ^{13}C . The 2D gs-DQF-COSY spectrum was recorded in
322 magnitude mode at 70°C. TOCSY experiments were recorded with variable mixing
323 times (60, 90, 120 ms). The 2D-heteronuclear ^1H - ^{13}C HSQC, and phase sensitive
324 HSQC-TOCSY were recorded using Bruker pulse sequences and 256 experiments
325 of 1024 data points. The NOESY spectrum was recorded using a Bruker pulse
326 sequence and 256 experiments of 1024 data points were recorded using a mixing
327 time of 200 ms. For the majority of spectra, time-domain data were multiplied by
328 phase-shifted (squared-) sine-bell functions. After applying zero-filling and Fourier
329 transformation, data sets of 1024-1024 points were obtained.

330 A mild acid hydrolysis treatment of the HMW-EPS was carried out as follows:
331 a solution of EPS (10 mg mL $^{-1}$) was mixed with 20 μl of TFA in an NMR tube and
332 kept at 70°C for 24 h. Hydrolysis was monitored by ^1H NMR, spectra were recorded
333 every hour for first 8 h and then after 24 h.

334 **3.4. Sequencing of the putative eps cluster of *B. animalis* subsp. *lactis* IPLA-R1**

335 Strain *B. animalis* subsp. *lactis* IPLA-R1 was grown for 24 h in 10 mL of
336 MRSC broth to isolate DNA using the "GenElute Bacterial Genomic DNA" kit (Sigma)
337 following the manufacturer instructions, but including a previous step of bacterial
338 lysis with mutanolysin and lysozyme⁸. For sequencing the putative *eps* cluster, 54

339 pair of PCR primers were designed taking into account the sequence of the type
340 strain *B. animalis* subsp. *lactis* DSM10140, whose genome is publicly available
341 (GenBank accession number CP001606)²⁴. Primers, synthesised by Thermo-Fisher
342 Scientific GmbH (Ulm, Germany), amplified regions of about 1,000 bp. The PCR
343 reaction mixture in a final volume of 50 µl was: 1 µl chromosomal DNA, 0.20 µM of
344 each primer, 200 µM dNTPs (Amersham Bioscience, Upsala, Sweden) and 2.5 U
345 Taq DNA-polymerase (Eppendorf, Hamburg, Germany). The PCR thermal conditions
346 were an initial denaturalisation cycle 95°C for 5 min, 30 amplification cycles of: 95°C
347 for 1 min, 52 or 56°C (variable according to the pair of primers) for 50 s and 68°C for
348 2 min, and a final extension step of 68°C for 10 min. Amplification was done in a
349 UnoCycler thermal cycler (VWR International Eurolab S.L., Barcelona, Spain). PCR
350 amplified products were visualised under UV in 1% agarose gels, after staining with
351 ethidium bromide. Purification and sequencing of each amplicons (both strands) was
352 performed by Macrogen (Seoul, Korea). Sequences obtained were processed with
353 the free Chromas 1.45 software (Technelysium Pty Ltd., Australia) and used for
354 comparison with those held in the GenBank database
355 (<http://www.ncbi.nlm.nih.gov/genbank>) using the BLASTn and BLASTp tools.

356

357 **Acknowledgements**

358 This work was funded by the Spanish “Plan Nacional I+D+I” from the
359 “Ministerio de Ciencia e Innovación” (MICINN, FEDER funds from European Union)
360 through the project AGL2009-09445 and by the University of Huddersfield. C.
361 Hidalgo-Cantabrana acknowledges his FPI fellowship to MICINN.

362

363 **References**

- 364 (1) Margolles, A.; Mayo, B.; Ruas-Madiedo, P. Screening, identification and
365 characterization of *Lactobacillus* and *Bifidobacterium* strains. In *Handbook of*
366 *probiotics and prebiotics*, 2nd ed; Nomoto, K., Salmine, S., Lee, Y.K., Eds;
367 John Willey & Sons Inc.: New Jersey, **2009**; pp 4-43.
- 368 (2) FAO/WHO. Probiotics in foods. Health and nutritional properties and guidelines
369 for evaluation. In *FAO food and nutrition paper* No. 85 (ISBN 92-5-105513-0).
370 **2006**; pp 1-50.
- 371 (3) Mayo, B.; Delgado, S., Rodríguez, J.M.; Gueimonde, M.; *CAB Rev.*, **2008**, No.
372 055 (Online ISSN 1749-8848); pp 1-17.
- 373 (4) WGO. In *World Gastroenterology Organisation Practice Guidelines: Probiotics*
374 *and Prebiotics*
375 (http://www.worldgastroenterology.org/assets/downloads/en/pdf/guidelines/19_probio
376 [tics_prebiotics.pdf](http://www.worldgastroenterology.org/assets/downloads/en/pdf/guidelines/19_probiotics_prebiotics.pdf)) **2008**; pp 1-22.
- 377 (5) Ruas-Madiedo, P.; Abraham, A.; Mozzi, F.; de los Reyes-Gavilán, C.G.
378 Functionality of exopolysaccharides produced by lactic acid bacteria. In
379 *Molecular aspects of lactic acid bacteria for traditional and new applications*,
380 Mayo, B., López, P., Pérez-Martínez, G., Eds.; Research Signpost
381 Publishers: Kerala, India, **2008**; pp 137-166.
- 382 (6) Ruas-Madiedo, P.; Moreno, J.A.; Salazar, N.; Delgado, S.; Mayo, B.; Margolles,
383 A.; de los Reyes-Gavilán, C.G. *Appl. Environ. Microbiol.*, **2007**, *73*, 4385-
384 4388.

- 385 (7) Salazar, N.; Prieto, A.; Leal, J.A.; Mayo, B.; Bada-Gancedo, J.C.; de los Reyes-
386 Gavilán, C.G.; Ruas-Madiedo, P., *J. Dairy Sci.*, **2009**, *92*, 4158-4168.
- 387 (8) Ruas-Madiedo, P.; Gueimonde, M.; Arigoni, F.; de los Reyes-Gavilán, C.G.;
388 Margolles, A. *Appl. Environ. Microbiol.*, **2009**, *75*, 1204-1207.
- 389 (9) Salazar, N.; Gueimonde, M.; Hernández-Barranco, A.M.; Ruas-Madiedo, P.; de
390 los Reyes-Gavilán, C.G. *Appl. Environ. Microbiol.*, **2008**, *74*, 4737-4745.
- 391 (10) Salazar, N.; Binetti, A.; Gueimonde, M.; Alonso, A.; Garrido, P.; González del
392 Rey, C.; González, C.; Ruas-Madiedo, P.; de los Reyes-Gavilán, C.G., *Int. J.*
393 *Food Microbiol.*, **2011**, *144*, 342-351.
- 394 (11) Ruas-Madiedo, P.; Medrano, M., Salazar, N.; de los Reyes-Gavilán, C.G.;
395 Pérez, P.F.; Abraham, A. *J. Appl. Microbiol.*, **2010**, *109*, 2079-2086.
- 396 (12) Zdrovenko, E.L.; Kachala, V.V.; Sidarenka, A.V.; Izhik, A.V.; Kisileva E.P.;
397 Shashkov, A.S.; Novik, G.I.; Knirel, Y.A. *Carbohydr. Res.*, **2009**, *344*, 2417-
398 2420.
- 399 (13) Kohno, M.; Suzuki, S.; Kanaya, T.; Yoshino, T.; Matsuura, Y.; Asada, M.;
400 Kitamura, S., *Carbohydr. Polym.*, **2009**, *77*, 351-357.
- 401 (14) Lee, J.H.; O'Sullivan, J., *Microbiol. Mol. Biol. Rev.*, **2010**, *74*, 378-416.
- 402 (15) Harding, L. P.; Marshall, V. M.; Hernandez, Y.; Gu, Y. C.; Maqsood, M.; McLay,
403 N.; Laws, A. P. *Carbohydr. Res.*, **2005**, *340*, 1107-1111.
- 404 (16) Carpita, N.C.; Shea, E.M. Linkage Structure Of Carbohydrates By Gas-
405 Chromatography - Mass Spectrometry Of Partially Methylated Alditol

- 406 Acetates. In *Analysis of Carbohydrates by GLC and MS*. Bierman C.J.;
407 McGinnis G.D. Eds.; CRC Press: Florida, USA, **1988**; pp 157-216.
- 408 (17) Briczinski, E.P.; Loquasto, J.R.; Barrangou, R.; Dudley, E.G.; Roberts, A.M.;
409 Roberts, R.F., *Appl. Environ. Microbiol.*, **2009**, *75*, 7501-7508.
- 410 (18) Ruas-Madiedo, P.; Salazar, N.; de los Reyes-Gavilán, C.G. Biosynthesis and
411 chemical composition of exopolysaccharides produced by lactic acid bacteria.
412 In *Bacterial polysaccharides: current innovations and future trends*. Ullrich, M.,
413 Ed.; Caister Academic Press: Norfolk, UK, **2009**; pp 279-310.
- 414 (19) Schell, M.A., Karmirantzou, M., Snell, B.; Vilanova, D.; Berger, B.; Pessim G.;
415 Zwahlen, M.C.; Desiere, F.; Bork, P.; Delley, M.; Pridmore, R.D.; Arigoni, F.
416 *PNAS*, **2002**, *99*, 14422-14427.
- 417 (20) van Calsteren, M.R.; Pau-Roblot, C.; Begin, A.; Roy, D., *Biochem. J.*, **2002**, *363*,
418 7-17.
- 419 (21) Péant, B.; LaPointe, G.; Gilbert, C.; Atlan, D.; Ward, P.; Roy, D., *Microbiology*,
420 **2005**, *151*, 1839-1851.
- 421 (22) Gerwig, G. J.; Kamerling, J. P.; Vliegthart, J. F. G. *Carbohydr. Res.* **1978**, *62*,
422 349-357.
- 423 (23) Stellner, K.; Saito, H.; Hakomori, S. I. *Arch. Biochem. Biophys.* **1973**, *155*, 464-
424 472.
- 425 (24) Barrangou, R.; Briczinski, E.P.; Traeger, L.L.; Loquasto, J.R.; Richards, M.;
426 Hovath, P.; Coûte; Monvoisin, A.C.; Leyer, G.; Rendulic, S.; Steele, J.L.;

427 Broadbent, J.R.; Oberg, T.; Dudley, E.G.; Schuster, S.; Romero, D.A.;
428 Roberts, R.F., *J. Bacteriol.*, **2009**, *191*, 4144-4151.

429

430

431 **Figure Legends**

432

433 **Figure 1** 500 MHz ^1H NMR spectrum of the HMW-EPS obtained after separation of
434 crude-EPS by dialysis in a 100 kDa cellulose acetate membrane; spectra recorded in
435 D_2O at 70°C . Inset shows an expanded plot of the anomeric region.

436

437 **Figure 2** (a): 500-MHz ^1H - ^{13}C HSQC spectrum of a selected region of the HMW-
438 EPS from *B. animalis* subsp. *lactis* IPLA-R1 recorded in D_2O at 70°C . The identity of
439 the cross peaks is noted by the sugar residue (**A-F**) and by identifying the location of
440 hydrogens/carbons within the ring as **2-5**. (b): anomeric region of the 500-MHz ^1H -
441 ^{13}C HSQC spectrum.

442

443 **Figure 3:** 500-MHz ^1H - ^1H NOESY spectrum of a selected region of the HMW-EPS
444 from *B. animalis* subsp. *lactis* IPLA-R1 recorded in D_2O at 70°C . The identity of the
445 cross peaks is noted by the sugar residue (**A-F**) and by identifying the location of
446 hydrogens within the ring as **1-5**. Intra-residue couplings are highlighted in red and
447 inter-residue couplings are highlighted in yellow. For interpretation of the references
448 to colour in this figure legend, the reader is referred to the web version of this article.

449

450 **Figure 4:** 500-MHz ^1H - ^{13}C HMBC spectrum of a selected region of the HMW-EPS
451 from *B. animalis* subsp. *lactis* IPLA-R1 recorded in D_2O at 70°C . The identity of the

452 cross peaks is noted by the sugar residue (A–D) and by identifying the location of
453 hydrogens within the ring as 1–5. Intra-residue couplings are highlighted in red and
454 inter-residue couplings are highlighted in yellow. (For interpretation of the references
455 to colour in this figure legend, the reader is referred to the web version of this article).
456

457 **Figure 5:** 500 MHz ^1H NMR spectra of the anomeric region following the acid
458 catalysed hydrolysis of the HMW-EPS from *B. animalis* subsp. *lactis* IPLA-R1 as a
459 function of time; spectra were recorded in D_2O at 70°C and the sample was
460 maintained at 70°C for the full reaction period. Sugar residues in the native HMW-
461 EPS are identified at the bottom (**A to F**), whereas those of the hydrolysed sample
462 are identified at the top (**A' to F'**).

463

464 **Figure 6:** Physical map of the putative *eps* cluster (54,259 bp) of *B. animalis* subsp.
465 *lactis* IPLA-R1. Predicted protein functions are categorised as follows: **GTF**,
466 glycosyltransferase; **p-GTF**, priming-GTF/ undecaprenyl-phosphate sugar
467 phosphotransferase / galactosyltransferase (CpsD); **Rh-B**, rhamnose biosynthesis
468 precursors; **P-ChL**, polymerization (polymerase) – chain length determination; **P-E**,
469 polymerization – export (Wzx and Wzz flippases); **PB**, polysaccharide biosynthesis;
470 **AcS**, acyl-synthetase; **Ph**, phosphorilase; **MP**, membrane protein; **T-IS**, transposase
471 – IS mobile elements; White arrows without label indicate hypothetical proteins.

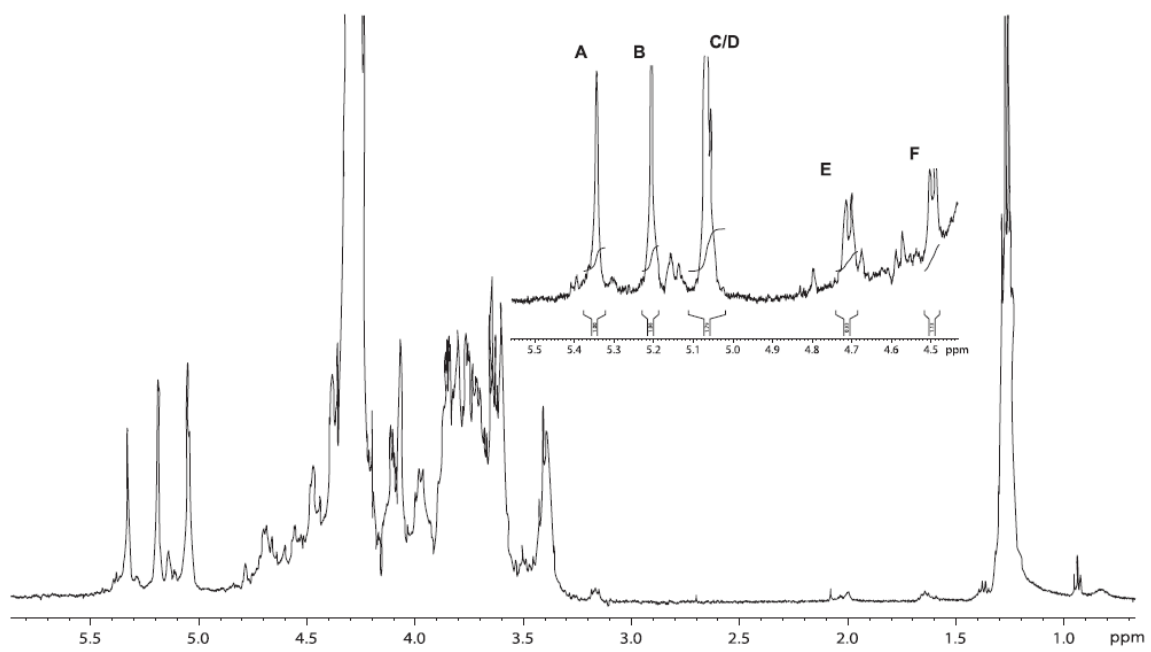
472

473 **Table 1:** ^1H and ^{13}C NMR chemical shifts of the HMW-EPS from *B. animalis* subsp.
474 *lactis* IPLA-R1 recorded in D_2O at 70°C

475

476 **Figure 1**

477



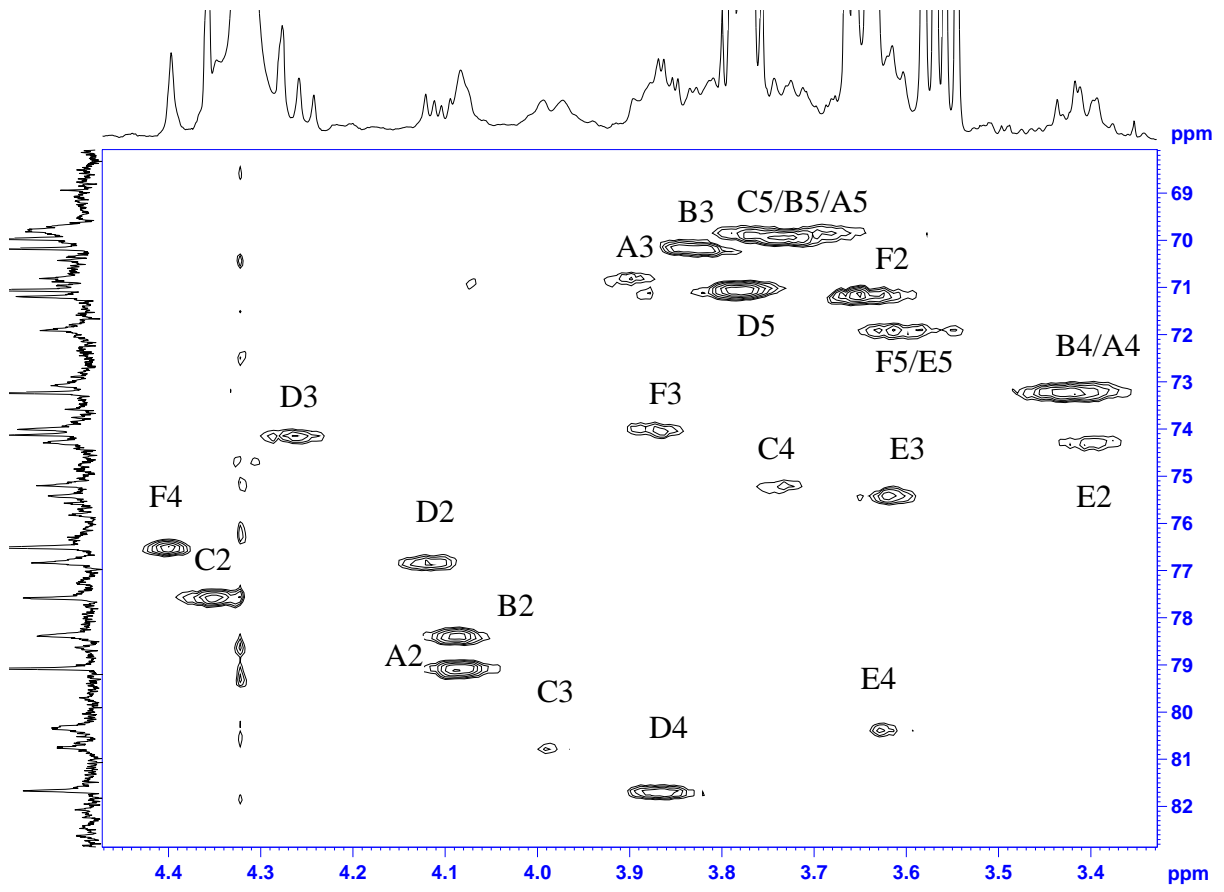
478

479

480

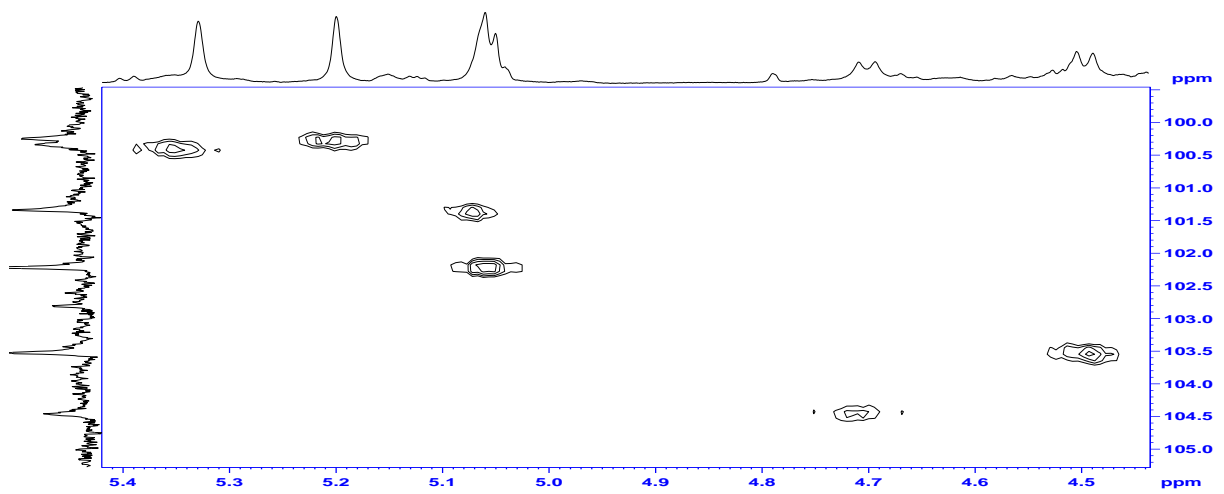
481 **Figure 2**

482 **a**



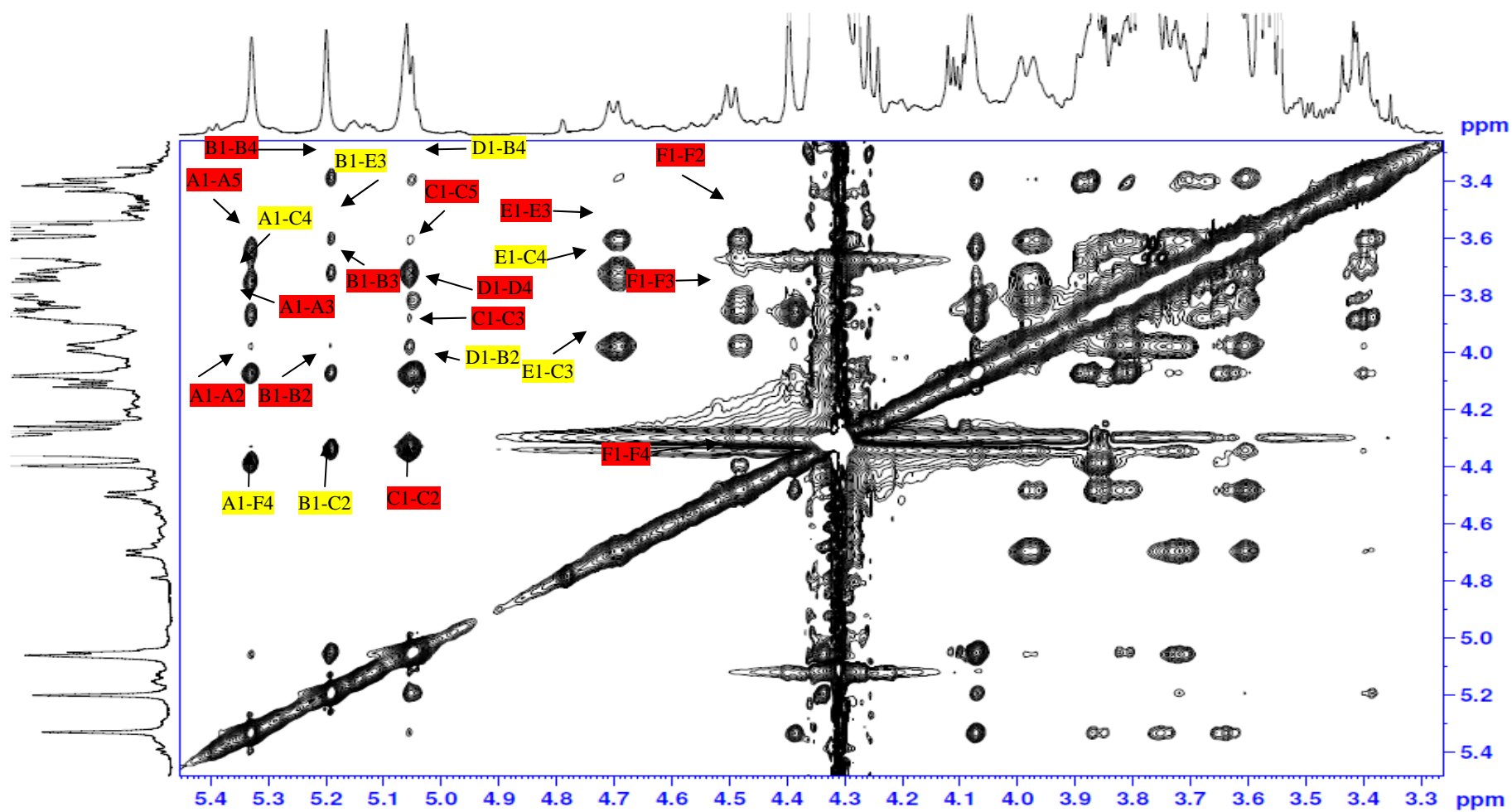
483

484 **b**



485
486

487 **Figure 3**



488

489

490

Figure 4

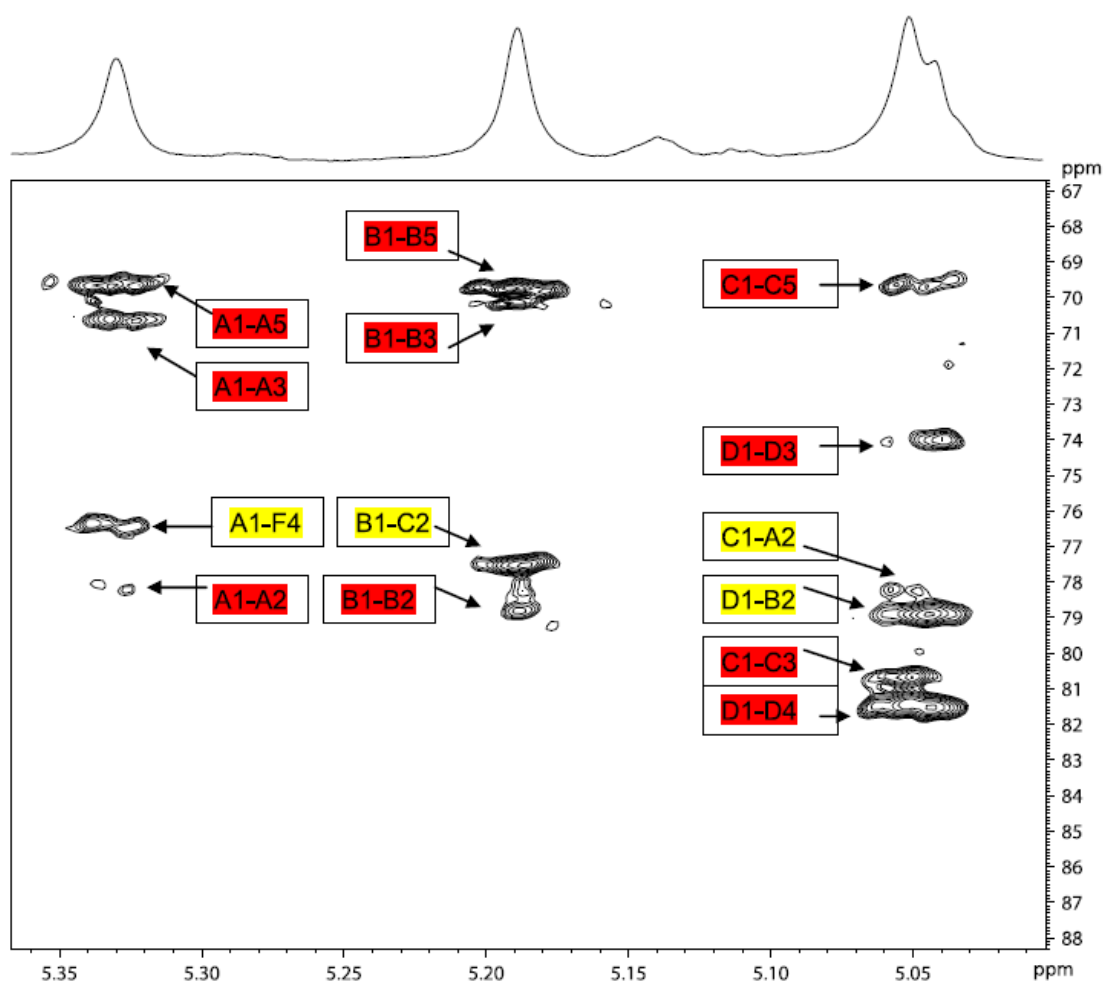


Figure 5

Figure 4

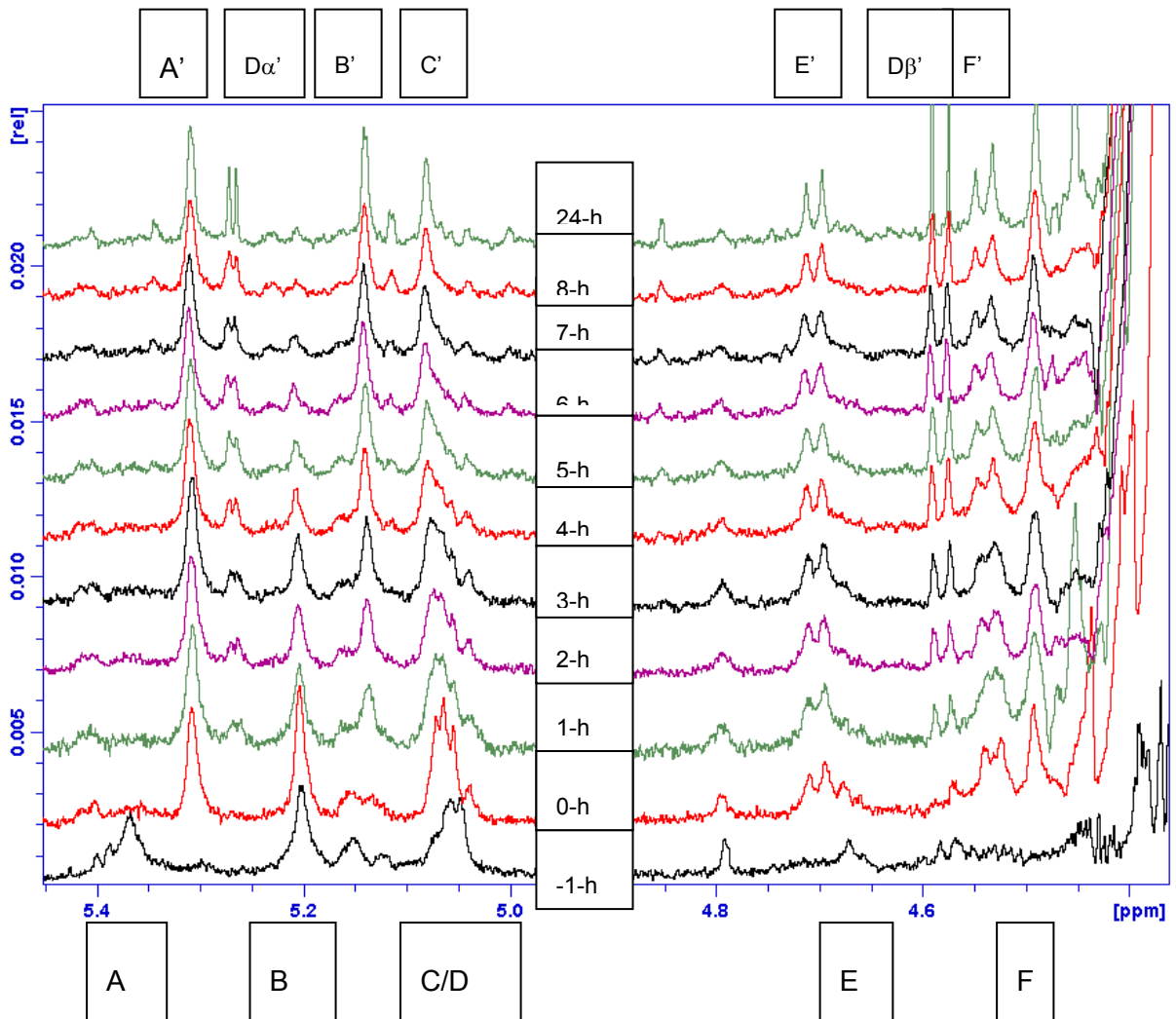
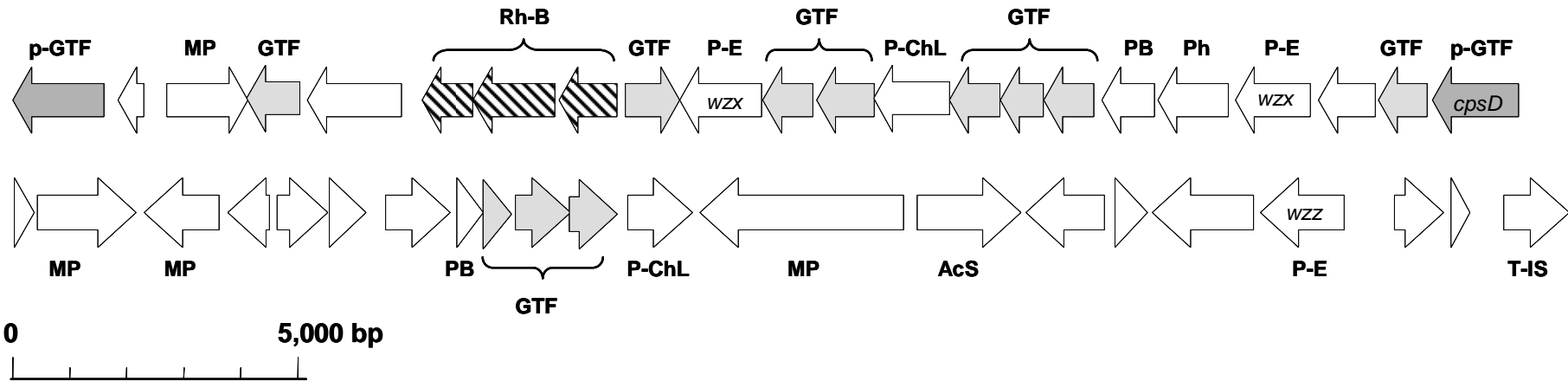


Figure 6



1 **Table 1**

2

Residue	¹ H Chemical Shift (ppm)							¹³ C Chemical Shift (ppm)					
	H1	H2	H3	H4	H5	H6	H6'	C1	C2	C3	C4	C5	C6
A	5.43	4.08	3.89	3.40	3.67	1.25	1.25	100.35	79.09	70.84	73.09	69.80	17.40
B	5.20	4.08	3.83	3.42	3.72	1.27	1.27	100.28	78.40	70.17	73.25	69.98	17.23
C	5.06	4.32	3.98	3.62	3.77	1.29	1.29	101.36	77.53	80.74	80.37	69.81	17.44
D	5.05	4.11	3.25	3.86	3.78	3.68*	3.90*	102.22	76.84	74.13	81.70	71.09	61.61
E	4.70	3.39	3.73	3.61	3.64	3.68*	3.90*	104.47	74.29	75.43	75.22	71.86	61.41
F	4.50	3.64	3.86	4.39	3.64	3.68*	3.90*	103.55	71.21	74.00	76.47	71.92	61.22

3 *Represents partially overlapping H6 and H6' resonances

4